In Vitro Autoradiography and In Vivo Evaluation in Cynomolgus Monkey of [^{18}F]FE-PE2I, a New Dopamine Transporter PET Radioligand

ANDREA VARRONE,[1,2]* CARSTEN STEIGER,[1] MAGNUS SCHOU,[1] AKIHIRO TAKANO,[1] SJOERD J. FINNEMA,[1] DENIS GUILLOTEAU,[3] BALÁZS GULYÁS,[1,2] AND CHRISTER HALLDIN[1,2]
[1]*Karolinska Institutet, Department of Clinical Neuroscience, Psychiatry Section, Stockholm, Sweden*
[2]*Stockholm Brain Institute, Stockholm, Sweden*
[3]*Inserm U930, Université François Rabelais de Tours, Tours, France*

KEY WORDS dopamine transporter (DAT); midbrain; substantia nigra; kinetics; metabolism

ABSTRACT This study evaluated the in vitro and in vivo characteristics of a new dopamine transporter (DAT) radioligand, [^{18}F]fluoroethyl(FE)PE2I, by autoradiography from postmortem human brain and by positron emission tomography (PET) in three cynomolgus monkeys. In the autoradiography experiments, high [^{18}F]FE-PE2I accumulation was observed in caudate and putamen that was selectively abolished by GBR12909 or β-CIT but not by maprotiline. High doses of citalopram (>5 μM) also inhibited [^{18}F]FE-PE2I binding in the striatum. In vitro K_i of the radioligand was 12 nM at rodent dopamine transporter. [^{18}F]FE-PE2I brain uptake measured by PET was ~4–5% of the injected dose, with highest uptake in striatum followed by midbrain and thalamus, lower uptake in neocortex, and lowest in cerebellum. Peak specific binding in striatum was reached ~40 min and in midbrain 20–30 min postinjection. The ratio-to-cerebellum was 7–10 in striatum and 1.5–2.3 in midbrain. BP_{ND} measured with simplified reference tissue method using the cerebellum as reference region was 4.5 in striatum and 0.6 in midbrain. No displacement was shown after citalopram or maprotiline administration, while GBR12909 decreased the binding in striatum and midbrain to the level of cerebellum. [^{18}F]FE-PE2I showed relatively fast elimination and metabolism with the presence of two metabolite peaks with similar retention time as the labeled metabolites of [^{11}C]PE2I. [^{18}F]FE-PE2I showed in vivo selectivity for the DAT and compared with [^{11}C]PE2I, it showed faster kinetics and earlier peak equilibrium. The potential influence of the two radiometabolites on PET quantification requires further evaluation. **Synapse 63:871–880, 2009.**

INTRODUCTION

Dopamine transporter (DAT) imaging is a well established tool for the evaluation of dopaminergic function in neurodegenerative disorders such as Parkinson's disease (PD) (Rinne et al., 1999) and in psychiatric disorders such as attention-deficit/hyperactivity disorder (ADHD) (Jucaite et al., 2005). Selective DAT radioligands with high affinity for the DAT and high in vivo target-to-background ratio permit visualization of not only the striatal DAT but also the midbrain/substantia nigra, where the cell bodies of the dopaminergic neurones are located. Imaging of the midbrain/substantia nigra has been shown to be relevant for studying the changes of the dopamine system in ADHD and might be important for the assessment of the dopaminergic deficit in PD, considering also the possibility to use a high-resolution PET system, such as the HRRT (Hirvonen et al., 2008; Leroy et al., 2007). At present, several radioligands labeled with either ^{11}C or ^{18}F are available (Halldin et al., 2001, 2003; Lundkvist et al., 1997; Saba et al., 2007;

Contract grant sponsor: EC; Contract grant numbers: FP6-Project DiMI, LSHB-CT-2005-512146.

Present address for Magnus Schou: Medicinal Chemistry AstraZeneca R&D, Södertäljie, Sweden

*Correspondence to: Andrea Varrone, Karolinska Institutet, Department of Clinical Neuroscience, Psychiatry Section, R5:02, Karolinska Hospital, SE-17176, Stockholm, Sweden. E-mail: andrea.varrone@ki.se

Received 28 October 2008; Accepted 27 January 2009

DOI 10.1002/syn.20670

Published online in Wiley InterScience (www.interscience.wiley.com).

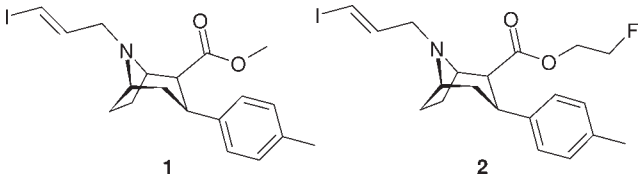

Fig. 1. Structures of PE2I (**1**) and FE-PE2I (**2**).

Yaqub et al., 2007). Among them the high-affinity DAT ligand (E)-*N*-(3-iodoprop-2-enyl)-2beta-carbomethoxy-3beta-(4′-methylphenyl)nortropane (PE2I, **1**, Fig. 1) (K_i = 17 nM) has been labeled both with ^{123}I and ^{11}C for SPECT and PET imaging (Halldin et al., 2003; Kuikka et al., 1998). [^{11}C]PE2I demonstrates a high in vivo specific-to-nondisplaceable ratio allowing the visualization of both striatum and midbrain/substantia nigra (Jucaite et al., 2006).

However, the slow kinetic properties of [^{11}C]PE2I in striatum are a relative limitation for accurate in vivo DAT quantification and at least one radiometabolite has been found to cross the blood brain barrier (BBB) in rat and to potentially interfere with the PET quantification (Shetty et al., 2007). While the metabolic fate of analogues of PE2I with similar chemical structure may not be different, chemical substitutions such as the addition of a fluoroalkyl group in the ester moiety could affect the brain kinetics of the radioligand, as for [^{11}C]FE-CIT vs. [^{11}C]β-CIT (Halldin et al., 1996). In addition, radiolabeling with ^{18}F could allow for longer imaging time and better quantification in both high- and low-density regions with different kinetic properties, respectively. The lower energy and the shorter positron range as compared with ^{11}C result in a better intrinsic resolution with ^{18}F, which could be an advantage for imaging and quantification of small brain regions such as the substantia nigra. Finally, labeling with ^{18}F would facilitate the production or distribution of the tracer in or to centers without the cyclotron, which could allow for a more widespread use of the tracer beyond specific research applications.

The aims of this study were as follows: (1) to evaluate the in vitro and in vivo characteristics of [^{18}F]FE-PE2I (**2**, Fig. 1) by autoradiography and PET imaging in nonhuman primates; and (2) to determine whether the addition of a fluoroethyl group in the ester moiety of PE2I would modify the metabolic pattern of the radioligand.

MATERIALS AND METHODS

Preparation of [^{18}F]FE-PE2I

[^{18}F]FE-PE2I was prepared from its acid precursor through the reaction with [^{18}F]2-bromo-1-fluoroethane in DMF (400 μl) and sodium hydroxide (5 M, 12 μl) in DMF (200 μl) as previously described (Schou et al., 2007). The overall radiochemical yield of [^{18}F]fluoroethyl bromide and [^{18}F]FE-PE2I based on [^{18}F]fluoride ion was 38 and 7%, respectively (uncorrected for decay). The range of specific radioactivity at time of injection was between 113 and 385 GBq/μmol.

In vitro binding assays

DAT affinity

The affinity of FE-PE2I for DAT was measured in competition studies using [^{125}I]PE2I. Briefly, a mixture of PE2I (4 nM), [^{125}I]PE2I (20 pM) and FE-PE2I at varying concentrations (10^{-6}, 10^{-10} M) was incubated with 30 μg of protein prepared from rat striatal membranes in a total volume of 1 ml in a Tris-HCl buffer, pH 7.4 (50 mM Tris-HCl, 120 mM NaCl, 5 mM KCl) at 22°C for 90 min. Nonspecific binding was measured with cocaine 30 μM. Samples were then filtered through Whatman GF/B filters soaked with 0.1% polyethylenimine (Sigma, St. Quentin-Fallavier, France) in cold buffer. The filters were washed twice with 4 ml of cold buffer, and the residual radioactivity was measured using a gamma counter (Cobra 5010, Packard).

IC_{50} values were determined graphically, and the K_i value was calculated assuming full competitive inhibition.

5-HTT affinity

The affinity of FE-PE2I for 5-HTT was measured in competition studies using [^{125}I]ADAM.

A mixture of ADAM (0.5 nM), [^{125}I]ADAM (25 pM) and FE-PE2I at varying concentrations (10^{-5}, 10^{-10} M) was incubated with 60 μg of protein prepared from rat cortical membranes in a total volume of 1 ml in a Tris-HCl buffer, pH 7.4 (50 mM Tris-HCl, 120 mM NaCl, 5 mM KCl) at 22°C for 90 min. Nonspecific binding was measured with ADAM 100 nM. Samples were then filtered and the residual radioactivity was measured as previously described.

IC_{50} values were determined graphically, and the K_i value was calculated assuming full competitive inhibition.

Autoradiography on postmortem human brain

Human brains were obtained from clinical autopsy at the National Institute of Forensic Medicine, Karolinska Institutet (Stockholm, Sweden) and handled in a similar manner as previously described (Hall et al., 1988, 1994). Cryosectioning on whole hemisphere sections was performed essentially as described previously (Hall et al., 1994). Horizontal sections (100 μm thick) containing caudate and putamen were used. The sections were incubated for 55 min at room temperature with 4 MBq [^{18}F]FE-PE2I in 200 ml of TRIS buffer (50 mM, pH 7.4) containing sodium chloride (100 mM) and 0.1% bovine serum albumin. The sec-

tions were then washed with the same buffer three times for 5 min each and briefly dipped in cold (+4°) distilled water. The imaging plates were scanned with a laser beam in the image-reading unit of the Phosphor Imager for 3 h (Fujifilm BAS-5000). Optical densities were analyzed using an image analysis program Multi Gauge V3.0. Coincubation experiments were performed with two DAT inhibitors, GBR 12909 and β-CIT (at concentration of 10 μM), one 5-HTT inhibitor, citalopram (1–20 μM), and one NET inhibitor, maprotiline (10 μM).

PET Measurements in cynomolgus monkeys

Three cynomolgus monkeys (*Macaca fascicularis*) (monkey 1: 9.3 kg, monkey 2: 6.2–7.35 kg, monkey 3: 3.9–4.5 kg) were examined in this study. The monkeys are owned by the Psychiatry Section, Department of Clinical Neuroscience, Karolinska Institutet and housed in the Astrid Fagraeus Laboratory of the Swedish Institute for Infectious Disease Control (SMI), Solna, Sweden. The study was approved by the Animal Ethics Committee of the Swedish Animal Welfare Agency and was performed according to "Guidelines for planning, conducting and documenting experimental research" (Dnr 4820/06-600) of the KI as well as the "Guide for the Care and Use of Laboratory Animals" (Clark et al., 1997). Anesthesia was induced and maintained by repeated intramuscular injections of a mixture of ketamine hydrochloride (3.75 mg/kg/h Ketalar® Pfizer) and xylazine hydrochloride (1.5 mg/kg/h Rompun® Vet., Bayer). The head was immobilized with a fixation device (Karlsson et al., 1993). Body temperature was maintained by Bair Hugger-Model 505 (Arizant Health Care, Inc., Minnesota) and monitored by an oral thermometer. ECG, heart rate, respiratory rate and oxygen saturation were continuously monitored throughout the experiments. Blood pressure was monitored every 15 min.

In vivo PET imaging was performed with the ECAT EXACT HR 47 (Siemens Medical Solutions) system. A 5 min transmission scan with three rotating ^{68}Ge sources was performed before each PET measurement. A total of seven PET measurements were conducted for 180 min with a series of frames of increasing duration (5 × 1 min, 5 × 3 min, 5 × 6 min, 13 × 10 min). Monkey 1 underwent only one baseline study (61 MBq). Monkey 2 underwent a baseline (59 MBq) plus two displacement studies performed with IV administration of either citalopram or maprotiline (5 mg/kg) 30 min after tracer injection (63 MBq, 56 MBq), and a pretreatment study with IV administration of citalopram (5 mg/kg) 20 min prior to tracer injection (66 MBq). Monkey 3 underwent a baseline study (59 MBq) plus a displacement study with IV administration of GBR 12909 (5 mg/kg) 10 min after tracer injection (67 MBq). Images were reconstructed with filtered back projection, using a 2-mm Hanning filter, a zoom factor of 2.17, and a 128 × 128 matrix and were corrected for attenuation and scatter (Wienhard et al., 1994).

Delineation of volumes of interest (VOIs) was guided by an atlas of a cryosected cynomolgus monkey head (Karlsson et al., 1993). VOIs for caudate, putamen, midbrain, thalamus, neocortex (average of frontal, temporal and occipital cortices), cerebellum, and whole brain, were drawn using the software PMOD (PMOD 2.65, PMOD Technologies, Zurich, Switzerland). The following procedure was used: first, VOIs for high density (putamen) and low density (cerebellum) regions were drawn on mean images from 11 to 180 min; second, time activity curves (TACs) generated from these regions were used as input data for pixel-wise modeling with multilinear reference tissue model 2 (MRTM2) using PMOD (Ichise et al., 2003); third, parametric images of R_1 (similar to blood flow) and BP_{ND} (Innis et al., 2007) were obtained. Finally, VOIs were drawn on combined R_1 and BP_{ND}/average images.

Volumes of VOIs were the following: Monkey 1: caudate, 0.52 cm^3, putamen 0.80 cm^3, midbrain 0.21 cm^3, thalamus 0.52 cm^3, neocortex 4.62 cm^3, cerebellum 1.12 cm^3, whole brain 77.7 cm^3; Monkey 2: caudate, 0.44 cm^3, putamen 0.80 cm^3, midbrain 0.23 cm^3, thalamus 0.67 cm^3, neocortex 4.94 cm^3, cerebellum 0.77 cm^3, whole brain 72.9 cm^3; Monkey 3: caudate, 0.39 cm^3, putamen 0.73 cm^3, midbrain 0.27 cm^3, thalamus 0.47 cm^3, neocortex 3.17 cm^3, cerebellum 0.83 cm^3, whole brain 59.4 cm^3. In monkey 2 an additional VOI of 0.21 cm^3 was drawn on the brainstem, to investigate the effect of citalopram pretreatment on a region with high density of 5-HTT.

In monkey 2 and 3 PET measurements were coregistered to each other by manual realignment of R_1 and BP_{ND} images using PMOD. Total brain uptake was calculated by multiplying the average radioactivity concentration from the whole brain VOI expressed as percentage of the radioactivity injected, by 65 ml which is the average volume of the brain of the cynomolgus monkey.

Decay corrected TACs for all regions were plotted over time. Cerebellum was considered as the reference region; the VOIs were drawn on cerebellar hemispheres, excluding the midline structure that could contain DAT binding sites (Melchitzky and Lewis, 2000). Specific binding was calculated as the difference between the radioactivity concentration in the target region and the cerebellum. The ratio of target-to-cerebellum was also plotted over time as relative affinity of the radioligand to the region comparing to the cerebellum. The quantitative outcome measure was BP_{ND} measured with the simplified reference tissue model (SRTM) using the cerebellum as reference region (Lammertsma and Hume, 1996). To investigate how the duration of the PET measurements would affect the esti-

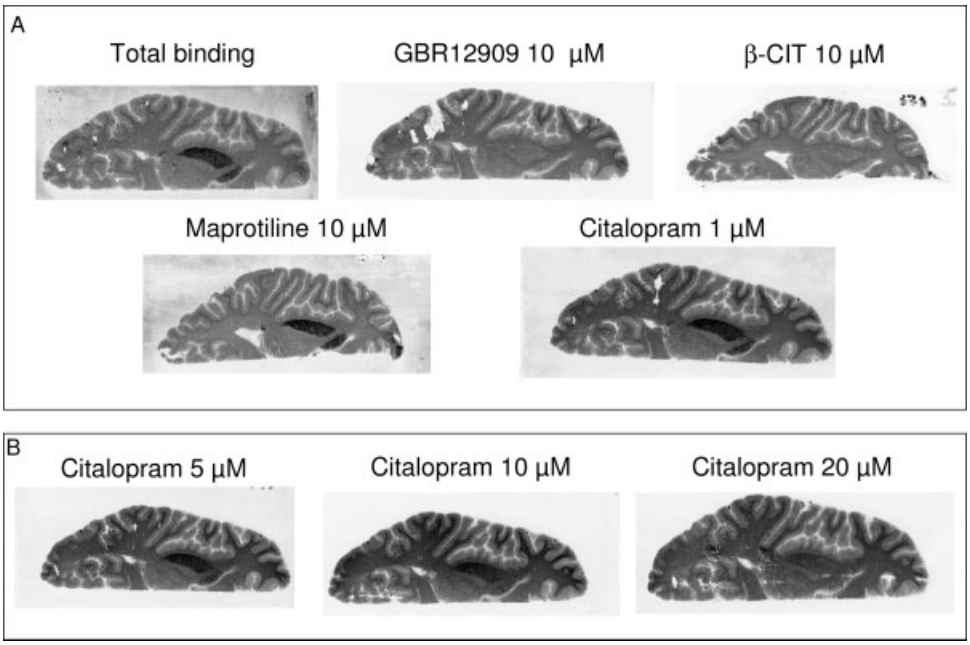

Fig. 2. In vitro autoradiography with [^{18}F]FE-PE2I on whole hemispheres from postmortem human brain, using 100 μm sections containing caudate and putamen. Complete blocking of [^{18}F]FE-PE2I was observed after coincubation with GBR12909 and β-CIT, but not with maprotiline or with citalopram at 1 μM concentration (**A**). However, a dose-dependent inhibition of [^{18}F]FE-PE2I binding was observed at concentrations of citalopram between 5 and 20 μM (**B**).

mate of BP_{ND}, PET data were progressively removed and BP_{ND} was calculated after 180, 130, 100, 70, and 50 min, respectively. The data were expressed as average BP_{ND} value ± average %COV of the estimate.

Metabolite analysis

A reverse phase high-performance liquid chromatography (HPLC) method was used to determine the percentages of radioactivity in monkey plasma that correspond to unchanged radioligand and radiometabolites during the course of a PET measurement (Halldin et al., 1995). Venous blood samples (2 ml) were obtained at 5, 15, 30, 45, 60, 90 and 180 min after injection of [^{18}F]FE-PE2I. Plasma (0.5 ml) obtained after centrifugation of blood at 2000*g* for 2 min was mixed with acetonitrile (0.7 ml). The supernatant acetonitrile-plasma mixture (1.1 ml) and the precipitate obtained after centrifugation at 2000*g* for 2 min were counted in a NaI well-counter. The well-counter consists of a NaI crystal (Harshaw, diameter: 38 mm × 50 mm; diameter of the well: 16 mm; depth: 38 mm). The crystal is housed inside a led shield cylinder with a wall thickness of ~5 cm. Furthermore the crystal is coupled to a high voltage supply, set to 900V (Canberra, model 3002), an energy descriminator (Canberra, model 818) and a timer and counter (GE&E Ortec, model 871).

The radio-HPLC system used in the plasma experiments consisted of an interface module (D-7000; Hitachi), a L-7100 pump (Hitachi), an injector (model 7125 with a 1.0 ml loop; Rheodyne) equipped with a μ-Bondapak-C18 column (300 × 7.8 mm, 10 μm; Waters) and an absorbance detector (L-7400; 254 nm; Hitachi) in series with a radiation detector (Radiomatic 150TR; Packard) equipped with a PET Flow Cell (600 μl cell). Acetonitrile (C) and phosphoric acid (10 mM) (D) were used as the mobile phase at 6.0 ml/min, according to the following program: 0–4.5 min, (C/D) 25:75 → 80:20 (v/v); 4.5–8.0 min, (C/D) 80:20 → 30:70 (v/v); 8.0–10.0 min, (C/D) 30:70 → 25:75 (v/v). Peaks for radioactive compounds eluting from the column were integrated and their areas expressed as a percentage of the sum of the areas of all detected radioactive compounds (decay-corrected).

To calculate the recovery of radioactivity from the system, an aliquot (2 ml) of the eluate from the HPLC column was measured for and divided with the amount of injected analyte.

RESULTS

In vitro binding assays

The K_i of FE-PE2I measured at rodent DAT and 5-HTT was 12 ± 1.7 nM (n = 3) and >1 μM (n = 3), respectively.

Autoradiography on postmortem human brain

The results of the autoradiographic studies with different blocking agents are shown in Figure 2. The

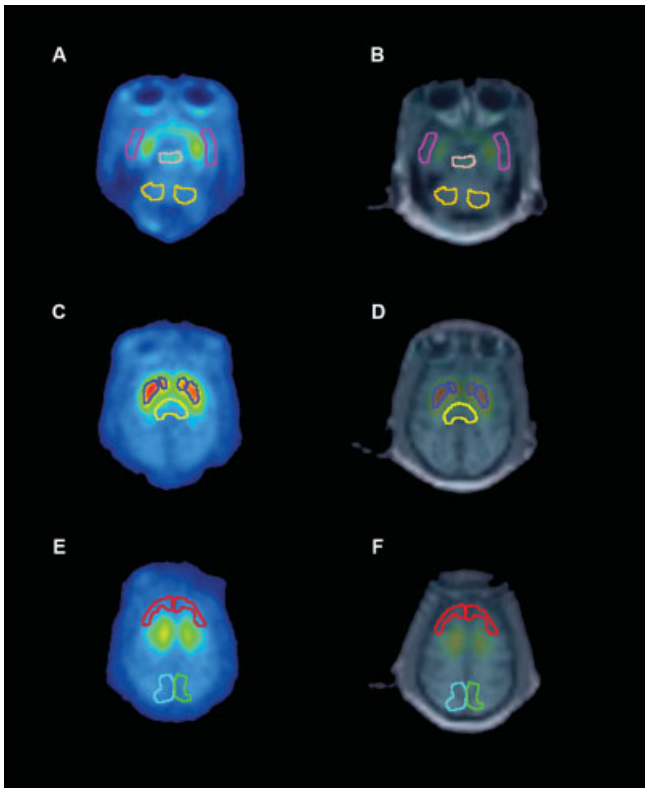

Fig. 3. PET images (**A**, **C**, **E**) and fused MR-PET images (**B**, **D**, **F**) of [18F]FE-PE2I showing the different VOIs delineated on A and B) cerebellum, temporal cortex, and midbrain; on C and D) caudate, putamen, and thalamus; E and F) frontal and occipital cortex.

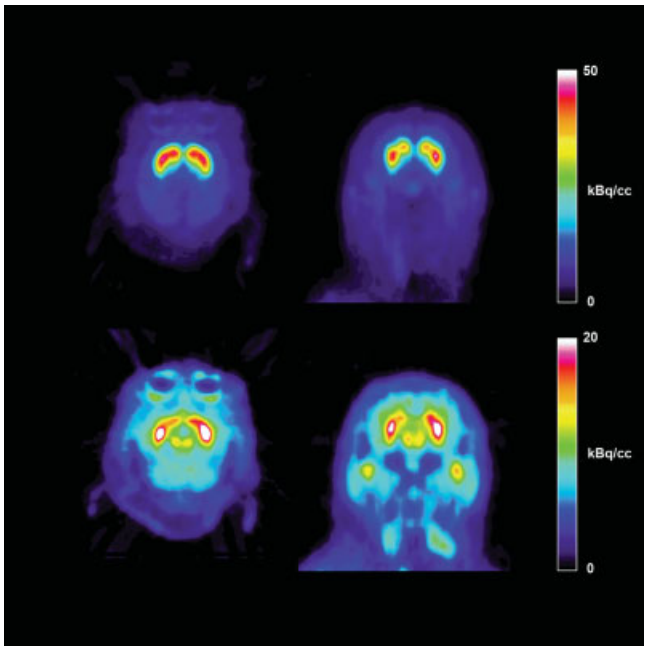

Fig. 4. Average images of [18F]FE-PE2I from 11 to 180 min after injection in monkey 1. Axial (left column) and coronal (right column) slices at the level of the striatum (upper row) and midbrain (lower row) are displayed. Not only the striatum, but also the midbrain/substantia nigra can be visualized. In the coronal section of the lower row, the activity seen below the two temporal lobes is due to uptake of the tracer by the salivary glands.

two DAT inhibitors GBR 12909 and β-CIT (10 μM) completely blocked the binding of the radioligand in the striatum. The NET inhibitor maprotiline at the concentration of 10 μM did not have any effect. The 5-HTT inhibitor citalopram did not show any effect at 1 μM concentration but did show a dose-dependent inhibition of [18F]FE-PE2I binding at concentrations from 5 to 20 μM.

PET measurements in cynomolgus monkeys

Images of the VOIs and of [18F]FE-PE2I in a cynomolgus monkey are shown in Figures 3 and 4. Two-to-three min after injection ~4–5% (400–500%SUV) of [18F]FE-PE2I reached the brain (Fig. 5A). The radioligand showed relatively fast wash-out with ~1% still present 90 min after injection. The highest uptake was observed in the caudate and the putamen, with a peak at ~12–15 min after injection, followed by lower uptake in the midbrain, the thalamus and the neocortex (Fig. 5B). The lowest uptake was observed in the cerebellum. Peak specific binding (region minus cerebellum) was reached in the striatum at 41–47 min and in the midbrain at 20–30 min postinjection (Fig. 5C). The ratio of uptake to the cerebellum was 7–10 in the striatum and 1.5–2.3 in the thalamus and the midbrain (Fig. 5D). BP_{ND} measured with SRTM was ~4.5 in striatum, 0.6 in midbrain and 0.4 in thalamus, consistent with the known relative brain distribution of the DAT (Table I). BP_{ND} was relatively stable in relation to the duration of PET data, with relatively low increase in the %COV of the estimate (Fig. 6). The average bias of BP_{ND} using 70 min of PET data was −4% in the caudate, −6% in the putamen, 4% in the midbrain and −2% in the thalamus. The average %COV of the estimate increased from 0.8% to 3.1% in the caudate, from 0.7% to 2.4% in the putamen, from 3.2% to 5.5% in the midbrain and from 4.2% to 6.3% in the thalamus, using 70 min of data acquisition.

The administration of 5 mg/kg of GBR 12909 10 min after injection determined a complete displacement of [18F]FE-PE2I from the striatum and the midbrain, with the radioactivity concentration reaching the value of the cerebellum at 180 min postinjection (Fig. 7A). No effect was seen in the cerebellum confirming its suitability as a reference region. No evident effect was seen when either maprotiline or citalopram were administered 30 min postinjection (Fig. 7B). The administration of citalopram 20 min before tracer injection was associated with an increase of [18F]FE-PE2I uptake in striatum, midbrain, brainstem and cerebellum (Fig. 7C). BP_{ND} estimated with

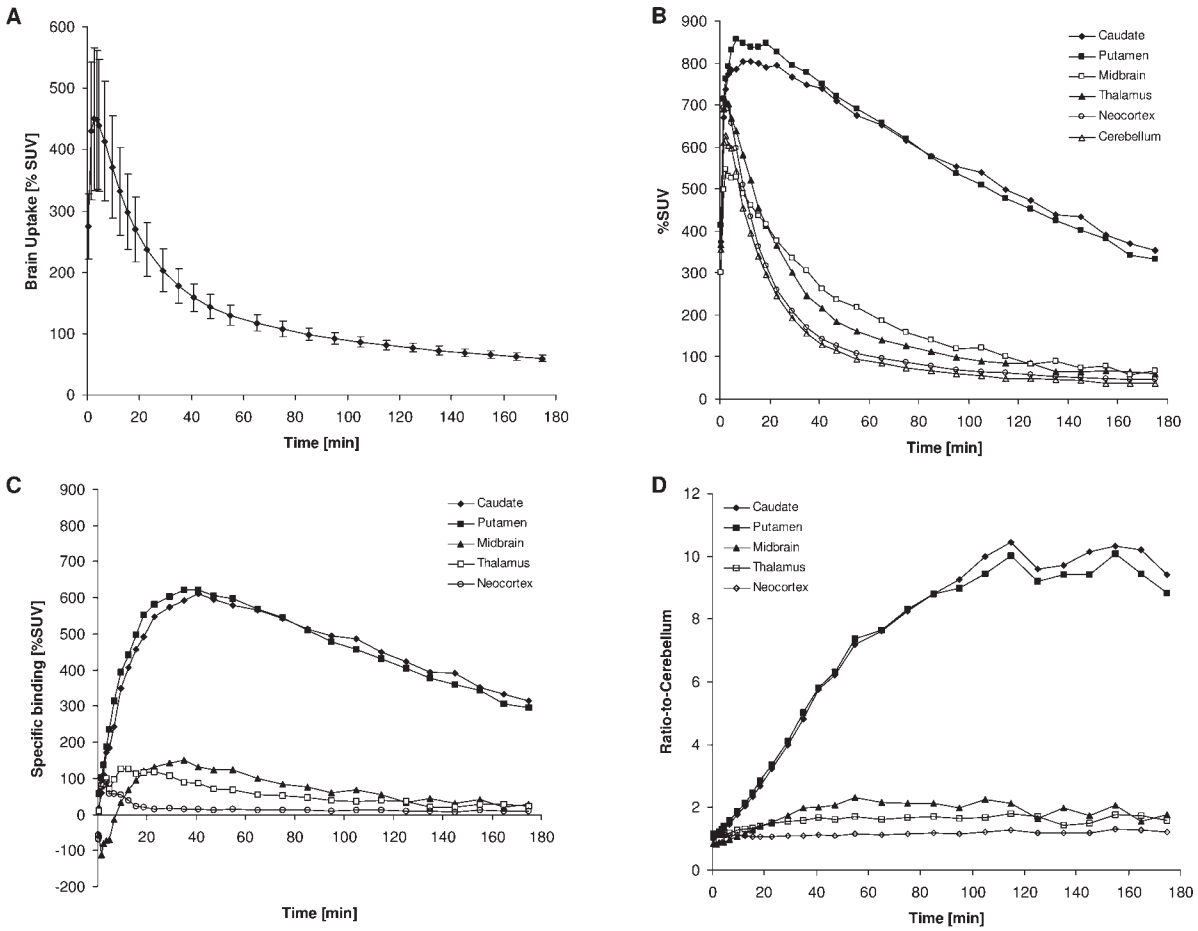

Fig. 5. Total brain uptake of [^{18}F]FE-PE2I expressed as percent standardized uptake value (%SUV) (mean ± SD from the three monkeys) (**A**). Time activity curves (**B**), specific binding (**C**), and ratio-to-cerebellum (**D**) of [^{18}F]FE-PE2I in different brain regions in monkey 1.

TABLE 1. BP_{ND} values for [^{18}F]FE-PE2I in the three cynomolgus monkeys examined, using SRTM and cerebellum as reference region

	Caudate	Putamen	Midbrain	Thalamus
Monkey 1	4.97	4.75	0.62	0.46
Monkey 2	4.11	4.36	0.64	0.56
Monkey 3	4.25	4.51	0.60	0.31
Mean ± SD	4.44 ± 0.46	4.54 ± 0.20	0.62 ± 0.02	0.44 ± 0.12

SRTM increased by 7.2% in the caudate (from 4.11 to 4.40), 7.8% in the putamen (from 4.36 to 4.70), 26.7% in the midbrain (from 0.64 to 0.81), and 11.8% in the brainstem (from 0.36 to 0.40). However, since the citalopram administration was associated with an increase of radioactivity in all brain regions, we also measured the ratio of the target region to the cerebellum between 110 and 180 min, as an estimate of the effect of the citalopram independently of differences in tracer delivery to the brain between baseline and pretreatment experiments. The ratio-to-cerebellum in baseline and pretreatment experiments was respectively: 7.21 and 7.21 in the caudate, 7.68 and 7.62 in the putamen, 1.36 and 1.54 in the midbrain, 1.28 and 1.24 in the brainstem.

Metabolite analysis

The recovery of radioactivity from plasma into acetonitrile after deproteinization was 96 ± 1% (n = 5). The corresponding recovery from the analytical system was 91 ± 13% (n = 5). [^{18}F]FE-PE2I showed relatively fast elimination and metabolism. At 15 min ~35% of the plasma radioactivity was unchanged parent radioligand, decreasing to 10% at 60 min postinjection (Fig. 8A).

HPLC analysis of plasma following injection of [^{18}F]FE-PE2I, which eluted at 5.5 min, revealed the presence of two major peaks, [^{18}F]**a** and [^{18}F]**b** with retention times of 3 and 4.5 min, respectively (Fig. 8B). [^{18}F]**a** was more abundant, representing ~60% of the plasma radioactivity at 45 min postinjection and with lower lipophilicity than the parent (as judged from its short retention time on HPLC). [^{18}F]**b** was less abundant (~18% of plasma radioactivity at 45

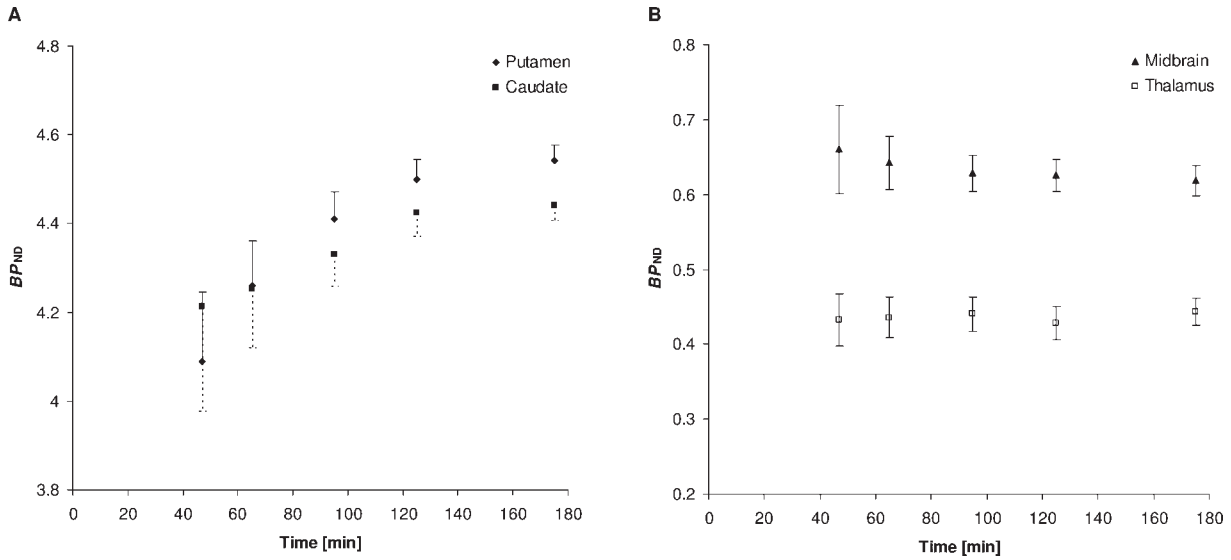

Fig. 6. Time dependency of BP_{ND} as a function of duration of PET measurement. Average BP_{ND} values and average %COV of the estimate for the three monkey examined are reported.

min postinjection), but with intermediate lipophilicity as compared with the parent and [18F]**a**.

DISCUSSION

In this study [18F]FE-PE2I, the new 18F-labeled fluoroethyl analog of PE2I, modified in the ester moiety, was evaluated to assess its suitability as a PET radioligand for the DAT. FE-PE2I showed similar potency at the DAT as PE2I (K_i = 12 vs. 17 nM for FE-PE2I and PE2I, respectively), which was expected and in line with previous results from modifications of the ester moiety in tropanes (Carroll et al., 1992, 1995).

PET measurements in cynomolgus monkeys indicated that [18F]FE-PE2I shows (1) fast kinetics, (2) earlier peak specific binding than [11C]PE2I (in striatum at ~40 min, in midbrain at ~20 min), (3) high specific-to-nondisplaceable binding ratio (BP_{ND} 4.5 in striatum and 0.6 in midbrain), and (4) in vivo selectivity for the DAT. These characteristics would suggest that [18F]FE-PE2I is a suitable radioligand for PET imaging of the DAT. As compared with [11C]PE2I there are also specific issues that should be considered.

Kinetic properties of [18F]FE-PE2I

The faster kinetics as compared with [11C]PE2I could be an advantage in terms of DAT quantification. The different kinetic behavior of the two radioligands could be related to possible differences between in vitro and in vivo conditions. The in vitro binding affinity (K_i) of the two radioligands is almost identical, which would lead to the assumption that also in vivo binding affinity (K_D) should be similar. However, in vitro K_D equals k_{off}/k_{on}, where in vitro k_{off} corresponds to in vivo k_4 and k_{on} is included in the in vivo k_3 as $k_3 = f_{ND}k_{on}B_{avail}$ [see (Innis et al., 2007)]. For several neuroreceptor ligands the in vivo rate of dissociation (k_4) is slower than the in vitro rate (k_{off}) and also k_3 appears to be similarly decreased so that the ratio k_3/k_4 is proportional to the in vivo K_D. One possibility could be that the addition of the fluoroethyl group in the ester moiety of PE2I could lead to a faster in vivo k_4 (although labeled in a different position this appears to be the case for [11C]FE-CIT, see Halldin et al., 1996) and that the in vivo k_3/k_4 ratio of [18F]FE-PE2I would be lower than [11C]PE2I, also resulting in a lower in vivo K_D. Kinetic modeling and comparison of rate constants and outcome measures with [11C]PE2I would allow to better clarify this issue.

The advantage of the faster kinetics is demonstrated by the fact that although we conducted PET measurements for 180 min, an evaluation of the time stability of BP_{ND} using SRTM has shown that 70 min of data acquisition would be adequate to obtain reliable estimate of DAT availability. Ketamine has been reported to affect the striatal dopaminergic system and to alter the binding of radioligands to the DAT (Tsukada et al., 2000). Therefore, it is possible that the ketamine/xylazine anesthesia could modify the kinetics of [18F]FE-PE2I and that in the awake conditions the kinetics of the radioligand would be different. The effect of anesthesia, however, is unlikely to affect the main findings of the study since all displacement and pretreatment experiments were performed under the same conditions of anesthesia.

In vitro/in vivo selectivity for the DAT

[18F]FE-PE2I appears to be selective for the DAT in vitro and in vivo. In vitro, FE-PE2I showed ~10,000-

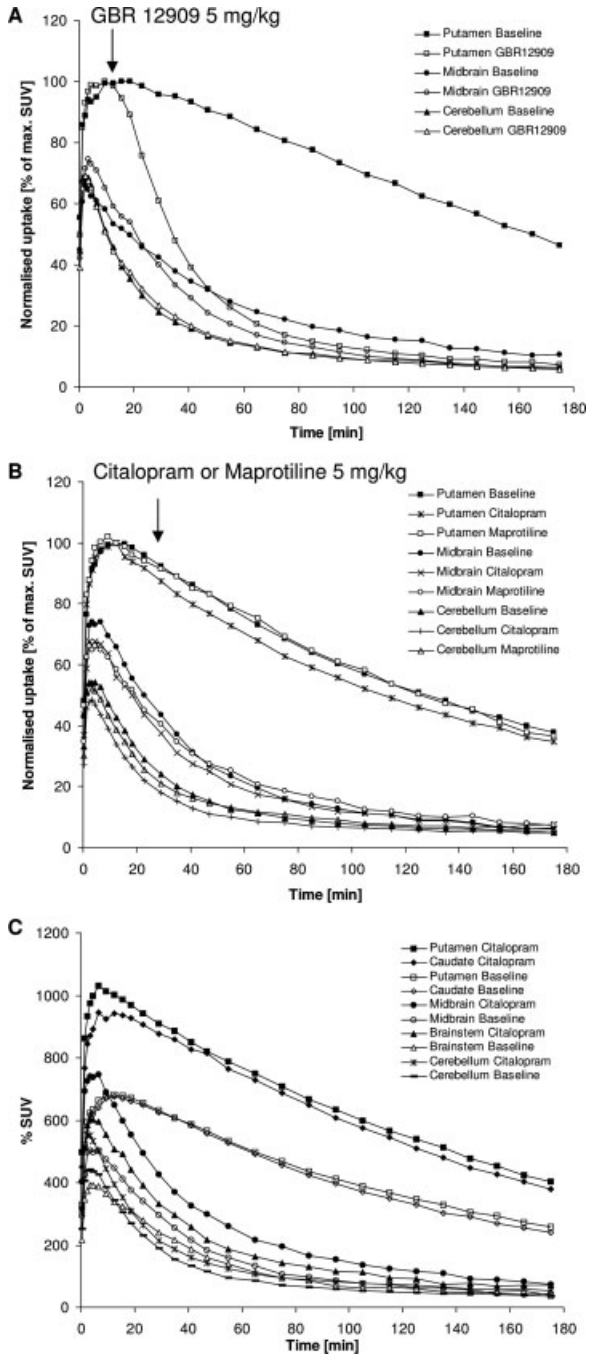

Fig. 7. Regional time activity curves from the baseline and displacement experiments with GBR12909 (10 min after tracer injection) in monkey 3 (**A**) from the baseline and displacement experiments with citalopram and maprotiline (30 min after tracer injection) in monkey 2 (**B**), and from the baseline and pretreatment experiment with citalopram (5 mg/kg IV, 20 min prior to tracer injection) in monkey 2 (**C**). Radioactivity is expressed as percentage of maximum SUV (A, B) or as %SUV (C).

higher selectivity for the DAT as compared with the 5-HTT. The autoradiography data showed a dose dependent effect of citalopram between 5 and 20 μM. The in vitro inhibition of [^{18}F]FE-PE2I binding might have been related to the pharmacological selectivity of citalopram since it occurred at concentration corresponding to the in vitro K_i of the 5-HTT inhibitor for the DAT (~20 μM) (Owens et al., 2001). A previous autoradiographic study with [^{125}I]PE2I showed no effect of citalopram at concentration up to 10 μM (Hall et al., 1999), thus a comparison of the two radioligands using the same experimental blocking conditions would be needed to evaluate whether citalopram had a different effect on FE-PE2I vs. PE2I, but this was beyond the scope of the present study.

In the present study no effect of citalopram on [^{18}F]FE-PE2I binding has been shown in in vivo displacement experiments at doses (5 mg/kg) ~20 times higher than the dose used clinically (0.2–0.3 mg/kg) and known to yield ~80% occupancy of the 5-HTT (Lundberg et al., 2007), suggesting in vivo selectivity of the tracer for the DAT.

In the pretreatment experiment with citalopram there was an increase in BP_{ND} in both striatum, midbrain, and brainstem. However, the uptake of the radioligand in target and reference regions was increased in the pretreatment experiment. This increase can be explained by differences in the delivery of the tracer to the brain, for instance caused by a peripheral redistribution of the radioligand (Helfenbein et al., 1999), and by differences in DAT density, or by the combination of both mechanisms. We calculated the target-to-cerebellum ratio in the last 70 min of data acquisition to examine whether there was a difference between baseline and pretreatment experiments, independently of differences in the delivery of the tracer to the brain. We could not see any differences between baseline and pretreatment in the striatum and brainstem, and only a slight increase of 13% in the midbrain. Therefore, it is possible that the increase in BP_{ND} estimate in the citalopram experiment was influenced by changes in tracer kinetics independently of changes in DAT density. On the other hand, changes in DAT density cannot be ruled out. Previous ex vivo and in vivo studies have shown an increase in DAT availability within the range observed in this study, using different 5-HTT inhibitors administered either chronically or shortly before tracer injection (Fujita et al., 1997; Kugaya et al., 2003; Scheffel et al., 1994). One proposed explanation for this increase is that inhibition of 5-HT uptake could lead to a rapid regulation of DAT molecules to more efficiently remove DA from the synapse (Fujita et al., 1997; Kugaya et al., 2003). The mechanism by which elevated DAT binding after 5-HTT inhibition occurs is still unknown and requires further examination. Nevertheless, a possible increase in DAT binding of [^{18}F]FE-PE2I after citalopram administration would be in line with previous findings with other DAT radioligands and would not be explained by low selectivity of the radioligand.

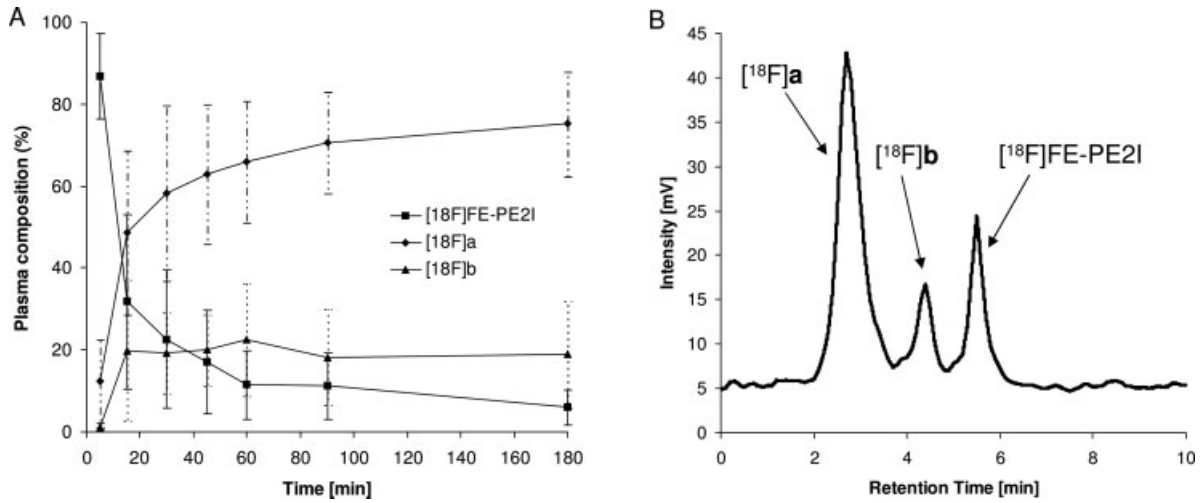

Fig. 8. In vivo metabolism of [18F]FE-PE2I. Mean ± SD of the relative composition as percentage of total plasma radioactivity from 5 to 180 min after injection in the three monkeys (**A**) and a representative HPLC chromatogram 45 min after injection (**B**). Two radiometabolite peaks were present, with similar retention time as those of [11C]PE2I, which we assumed are the equivalent 4-carboxyl- ([18F]**a**) and 4-hydroxymethyl- ([18F]**b**) analogues.

Metabolism of [18F]FE-PE2I

[18F]FE-PE2I showed similar pattern of metabolism as [11C]PE2I giving two HPLC peaks with less lipophilicity than parent ([18F]**a**) and with intermediate lipophilicity ([18F]**b**). The two radiometabolites of [11C]PE2I have been extensively studied in rodents and have been found to correspond to a 4-hydroxymethyl- ([11C]**1**) and a 4-carboxyl-([11C]**2**) analog of [11C]PE2I. In rodents, [11C]**1** has been found to cross the BBB and to accumulate in the striatum, while [11C]**2** is probably produced from [11C]**1** in the brain (Shetty et al., 2007). This last metabolite has been found mostly in the rodent cerebellum, therefore it seems to lack affinity for the DAT. The production of these two radiometabolites is likely to affect PET quantification. In the present study we assume that [18F]**b** and [18F]**a** are the equivalent 4-hydroxymethyl- and 4-carboxyl- analogs as in the case [11C]PE2I. Similarly as [11C]PE2I these two radiometabolites, and particularly the one with intermediate lipophilicity, would affect DAT quantification. However, a preliminary comparison of [18F]FE-PE2I and [11C]PE2I (data not shown) suggests that the metabolism of [18F]FE-PE2I is more favorable with less abundance of the metabolite with intermediate lipophilicity, which could be advantageous in terms of DAT quantification (Varrone et al., 2008).

It has been shown that for another DAT radioligand [18F]FECNT there is a polar radiometabolite [18F]fluoroethanol that crosses the BBB determining obvious effects on the cerebellar TAC (Zoghbi et al., 2006). However, in case of [11C]PE2I, only a minor portion is metabolized by ester hydrolysis (Shetty et al., 2007); if it also applies to [18F]FE-PE2I, then the contribution of [18F]fluoroethanol would be negligible. This is also suggested by the fact that we could not see any obvious effect on the cerebellar TAC of [18F]FE-PE2I.

CONCLUSIONS

[18F]FE-PE2I is a promising radioligand for in vivo imaging of the DAT. However, additional in vivo evaluation in nonhuman primates, including kinetic modeling and direct comparison of the metabolism with [11C]PE2I, is warranted before the tracer could be applied to human subjects.

ACKNOWLEDGMENTS

The authors thank members of the Karolinska Institutet PET Center for assistance in the PET experiments. They also thank Siv Eriksson for excellent technical assistance with the autoradiography experiments.

REFERENCES

Carroll FI, Abraham P, Lewin AH, Parham KA, Boja JW, Kuhar M. 1992. Isopropyl and phenyl esters of 3 beta-(4-substituted phenyl)-tropan-2 beta-carboxylic acids. Potent and selective compounds for the dopamine transporter. J Med Chem 35:2497–2500.

Carroll FI, Kotian P, Dehghani A, Gray JL, Kuzemko MA, Parham KA, Abraham P, Lewin AH, Boja JW, Kuhar MJ. 1995. Cocaine and 3 beta-(4′-substituted phenyl)tropane-2 beta-carboxylic acid ester and amide analogues. New high-affinity and selective compounds for the dopamine transporter. J Med Chem 38:379–388.

Clark JD, Gebhart GF, Gonder JC, Keeling ME, Kohn DF. 1997. Special report: The 1996 guide for the care and use of laboratory animals. Ilar J 38:41–48.

Fujita M, Takatoku K, Matoba Y, Nishiura M, Kobayashi K, Inoue O, Nishimura T. 1997. Enhancement of [123I]beta-CIT binding in

the striatum with clomipramine: is there a serotonin-dopamine interaction? Eur J Nucl Med 24:403–408.
Hall H, Farde L, Sedvall G. 1988. Human dopamine receptor subtypes–in vitro binding analysis using 3H-SCH 23390 and 3H-raclopride. J Neural Transm 73:7–21.
Hall H, Sedvall G, Magnusson O, Kopp J, Halldin C, Farde L. 1994. Distribution of D1- and D2-dopamine receptors, and dopamine and its metabolites in the human brain. Neuropsychopharmacology 11:245–256.
Hall H, Halldin C, Guilloteau D, Chalon S, Emond P, Besnard J, Farde L, Sedvall G. 1999. Visualization of the dopamine transporter in the human brain postmortem with the new selective ligand [125I]PE2I. Neuroimage 9:108–116.
Halldin C, Swahn C-G, Farde L, Sedvall G. 1995. Radioligand disposition and metabolism. Key information in early drug development. In: Comar D, ed. PET for drug development and evalution. Dordrecht: Kluwer Academic. pp. 55–65.
Halldin C, Farde L, Lundkvist C, Ginovart N, Nakashima Y, Karlsson P, Swahn CG. 1996. [11C]beta-CIT-FE, a radioligand for quantitation of the dopamine transporter in the living brain using positron emission tomography. Synapse 22:386–390.
Halldin C, Gulyas B, Langer O, Farde L. 2001. Brain radioligands–state of the art and new trends. Q J Nucl Med 45:139–152.
Halldin C, Erixon-Lindroth N, Pauli S, Chou YH, Okubo Y, Karlsson P, Lundkvist C, Olsson H, Guilloteau D, Emond P, Farde L. 2003. [(11)C]PE2I: a highly selective radioligand for PET examination of the dopamine transporter in monkey and human brain. Eur J Nucl Med Mol Imaging 30:1220–1230.
Helfenbein J, Loc'h C, Bottlaender M, Emond P, Coulon C, Ottaviani M, Fuseau C, Chalon S, Guenther I, Besnard JC, Frangin Y, Guilloteau D, Maziere B. 1999. A selective radiobrominated cocaine analogue for imaging of dopamine uptake sites: pharmacological evaluation and PET experiments. Life Sci 65:2715–2726.
Hirvonen J, Johansson J, Teras M, Oikonen V, Lumme V, Virsu P, Roivainen A, Nagren K, Halldin C, Farde L, Hietala J. 2008. Measurement of striatal and extrastriatal dopamine transporter binding with high-resolution PET and [(11)C]PE2I: quantitative modeling and test–retest reproducibility. J Cereb Blood Flow Metab 28:1059–1069.
Ichise M, Liow JS, Lu JQ, Takano A, Model K, Toyama H, Suhara T, Suzuki K, Innis RB, Carson RE. 2003. Linearized reference tissue parametric imaging methods: application to [11C]DASB positron emission tomography studies of the serotonin transporter in human brain. J Cereb Blood Flow Metab 23:1096–1112.
Innis RB, Cunningham VJ, Delforge J, Fujita M, Gjedde A, Gunn RN, Holden J, Houle S, Huang SC, Ichise M, Iida H, Ito H, Kimura Y, Koeppe RA, Knudsen GM, Knuuti J, Lammertsma AA, Laruelle M, Logan J, Maguire RP, Mintun MA, Morris ED, Parsey R, Price JC, Slifstein M, Sossi V, Suhara T, Votaw JR, Wong DF, Carson RE. 2007. Consensus nomenclature for in vivo imaging of reversibly binding radioligands. J Cereb Blood Flow Metab 27: 1533–1539.
Jucaite A, Fernell E, Halldin C, Forssberg H, Farde L. 2005. Reduced midbrain dopamine transporter binding in male adolescents with attention-deficit/hyperactivity disorder: association between striatal dopamine markers and motor hyperactivity. Biol Psychiatry 57:229–238.
Jucaite A, Odano I, Olsson H, Pauli S, Halldin C, Farde L. 2006. Quantitative analyses of regional [11C]PE2I binding to the dopamine transporter in the human brain: a PET study. Eur J Nucl Med Mol Imaging 33:657–668.
Karlsson P, Farde L, Halldin C, Swahn CG, Sedvall G, Foged C, Hansen KT, Skrumsager B. 1993. PET examination of [11C]NNC 687 and [11C]NNC 756 as new radioligands for the D1-dopamine receptor. Psychopharmacology (Berl) 113:149–156.
Kugaya A, Seneca NM, Snyder PJ, Williams SA, Malison RT, Baldwin RM, Seibyl JP, Innis RB. 2003. Changes in human in vivo serotonin and dopamine transporter availabilities during chronic antidepressant administration. Neuropsychopharmacology 28:413–420.
Kuikka JT, Baulieu JL, Hiltunen J, Halldin C, Bergstrom KA, Farde L, Emond P, Chalon S, Yu M, Nikula T, Laitinen T, Karhu J, Tupala E, Hallikainen T, Kolehmainen V, Mauclaire L, Maziere B, Tiihonen J, Guilloteau D. 1998. Pharmacokinetics and dosimetry of iodine-123 labelled PE2I in humans, a radioligand for dopamine transporter imaging. Eur J Nucl Med 25:531–534.
Lammertsma AA, Hume SP. 1996. Simplified reference tissue model for PET receptor studies. Neuroimage 4(3 Part 1):153–158.
Leroy C, Comtat C, Trebossen R, Syrota A, Martinot JL, Ribeiro MJ. 2007. Assessment of 11C-PE2I binding to the neuronal dopamine transporter in humans with the high-spatial-resolution PET scanner HRRT. J Nucl Med 48:538–546.
Lundberg J, Christophersen JS, Petersen KB, Loft H, Halldin C, Farde L. 2007. PET measurement of serotonin transporter occupancy: a comparison of escitalopram and citalopram. Int J Neuropsychopharmacol 10:777–785.
Lundkvist C, Halldin C, Ginovart N, Swahn CG, Farde L. 1997. [18F] beta-CIT-FP is superior to [11C] beta-CIT-FP for quantitation of the dopamine transporter. Nucl Med Biol 24:621–627.
Melchitzky DS, Lewis DA. 2000. Tyrosine hydroxylase- and dopamine transporter-immunoreactive axons in the primate cerebellum. Evidence for a lobular- and laminar-specific dopamine innervation. Neuropsychopharmacology 22:466–472.
Owens MJ, Knight DL, Nemeroff CB. 2001. Second-generation SSRIs: human monoamine transporter binding profile of escitalopram and R-fluoxetine. Biol Psychiatry 50:345–350.
Rinne JO, Ruottinen H, Bergman J, Haaparanta M, Sonninen P, Solin O. 1999. Usefulness of a dopamine transporter PET ligand [(18)F]beta-CFT in assessing disability in Parkinson's disease. J Neurol Neurosurg Psychiatry 67:737–741.
Saba W, Valette H, Schollhorn-Peyronneau MA, Coulon C, Ottaviani M, Chalon S, Dolle F, Emond P, Halldin C, Helfenbein J, Madelmont JC, Deloye JB, Guilloteau D, Bottlaender M. 2007. [11C]LBT-999: a suitable radioligand for investigation of extrastriatal dopamine transporter with PET. Synapse 61:17–23.
Scheffel U, Kim S, Cline EJ, Kuhar MJ. 1994. Occupancy of the serotonin transporter by fluoxetine, paroxetine, and sertraline: in vivo studies with [125I]RTI-55. Synapse 16:263–268.
Schou M, Steiger C, Varrone A, Guilloteau D, Halldin C. 2009. Synthesis, radiolabeling and preliminary in vivo evaluation of [18F]FE-PE2I, a new probe for the dopamine transporter. Bioorganic & Medicinal Chemistry Letters (in press).
Shetty HU, Zoghbi SS, Liow JS, Ichise M, Hong J, Musachio JL, Halldin C, Seidel J, Innis RB, Pike VW. 2007. Identification and regional distribution in rat brain of radiometabolites of the dopamine transporter PET radioligand [11C]PE2I. Eur J Nucl Med Mol Imaging 34:667–678.
Tsukada H, Harada N, Nishiyama S, Ohba H, Sato K, Fukumoto D, Kakiuchi T. 2000. Ketamine decreased striatal [(11)C]raclopride binding with no alterations in static dopamine concentrations in the striatal extracellular fluid in the monkey brain: multiparametric PET studies combined with microdialysis analysis. Synapse 37:95–103.
Varrone A, Schou M, Steiger C, Takano A, Finnema S, Guilloteau D, Gulyas B, Halldin C. 2008. Direct comparison of [11C]PE2I and [18F]FE-PE2I dopamine transporter PET imaging in the rhesus monkey with the High-Resolution Research Tomograph, HRRT. Eur J Nucl Med Mol Imaging 35 (Suppl 2):S157.
Wienhard K, Dahlbom M, Eriksson L, Michel C, Bruckbauer T, Pietrzyk U, Heiss WD. 1994. The ECAT EXACT HR: performance of a new high resolution positron scanner. J Comput Assist Tomogr 18:110–118.
Yaqub M, Boellaard R, van Berckel BN, Ponsen MM, Lubberink M, Windhorst AD, Berendse HW, Lammertsma AA. 2007. Quantification of dopamine transporter binding using [18F]FP-beta-CIT and positron emission tomography. J Cereb Blood Flow Metab 27: 1397–1406.
Zoghbi SS, Shetty HU, Ichise M, Fujita M, Imaizumi M, Liow JS, Shah J, Musachio JL, Pike VW, Innis RB. 2006. PET imaging of the dopamine transporter with 18F-FECNT: a polar radiometabolite confounds brain radioligand measurements. J Nucl Med 47:520–527.